Full-Lagrangian Based Newton Scheme for Dynamic Analysis of Electrostatic MEMS

S. K. De* and N. R. Aluru**

Beckman Institute for Advanced Science and Technology
University of Illinois at Urbana-Champaign
405 N. Mathews Avenue, Urbana, IL 61801
* sde@uiuc.edu, ** aluru@uiuc.edu

ABSTRACT

A full-Lagrangian based Newton scheme for the dynamic analysis of MEMS is developed in this paper. In this scheme, both the mechanical and the electrical analysis is done on the original un-deformed geometry, unlike conventional semi-Lagrangian approaches which perform a mechanical analysis on the un-deformed geometry and the electrostatic analysis on the deformed geometry. The full-Lagrangian approach allows accurate computation of the inter-domain coupling term (mechanical to electrical) for the Jacobian-matrix of the Newton method which, otherwise, is a difficult task for the semi-Lagrangian methods. Dynamic characteristics of a transverse and a lateral comb drive have been simulated using the full-Lagrangian approach. Second super harmonic resonance is found to occur at half of the resonant frequency in these devices.

Keywords: MEMS-dynamics, full-Lagrangian-analysis, Newton-scheme, Comb-drives, Second-super-harmonic-resonance

1 INTRODUCTION

Dynamic characteristics of electrostatic MEMS like resonant frequency, frequency response curves, Q-factor are important as they have a significant impact in the operation of devices like capacitive switches, resonators, tunable capacitors, inductors and filters. In this paper, we develop a physical level simulation method for the dynamic analysis of MEMS based on a full Lagrangian description [1], [2] of both the mechanical and electrical domains. A Newton scheme is implemented to obtain a self-consistent solution at any given time instant. Conventional FEM/BEM methods for the electrostatic MEM analysis [3] use a semi-Lagrangian approach, where a mechanical analysis is performed on the undeformed geometry of the device using a Lagrangian approach while the electrostatic analysis is performed on the deformed geometry. Computing the inter-domain coupling term (mechanical to electrical) for the Jacobian-matrix of the Newton method is a difficult task for the semi-Lagrangian method. It has been computed indirectly using a matrix free approach [4] for the semi-Lagrangian method. The matrix free approach can be sensitive to the perturbation parameter used in the process thereby affecting the convergence rate. The full Lagrangian based Newton method can directly and accurately compute the inter-domain coupling (mechanical to electrical), making it more robust and efficient. The strong non-linear coupling between the mechanical and the electrical domains often reduces the convergence rate significantly of the relaxation scheme [4], [5] thereby indicating the need for Newton based methods. The semi-Lagrangian methods require re-meshing of the deformed surfaces and re-computation of the surface interpolation functions before each electrostatic analysis. These steps are eliminated in the full-Lagrangian approach as the analysis is done on the undeformed geometry, making it faster and more efficient [1].

Results obtained from the full-Lagrangian approach have been found to be in good agreement with published data. Dynamic analyses of a transverse comb drive and a lateral comb drive are done using the new approach. The frequency response curves of these devices have been simulated and second super harmonic resonance observed. The rest of the paper is outlined as follows: Section 2 presents the basic governing equations for nonlinear mechanical and electrostatic analysis and describes the algorithm for the full-Lagrangian based Newton scheme for MEM dynamic analysis, Section 3 presents the results and conclusions are presented in Section 4.

2 THEORY

Dynamic analysis of electrostatic MEMS requires a self-consistent solution of the coupled mechanical and electrical equations at each time step [4]. Figure 1 shows a typical MEM device - a deformable cantilever beam over a fixed ground plane. A potential difference V applied between the two conductors induces electrostatic charges on the surface of the conductors. The charge distribution depends on the relative position of the two conductors. These electrostatic charges give rise to electrostatic pressure, which acts normal to the surface of the conductors and deforms the beam. When the beam deforms, the charge redistributes on the surface of the conductors and, consequently, the resultant electrostatic forces and the deformation also change. Figure 1 shows

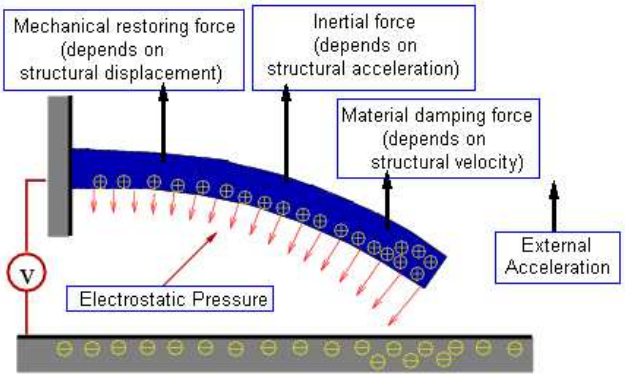

Figure 1: A cantilever beam over a ground plane: the deformed structure with charge redistribution and various forces acting on the structure at a time $t > 0$.

the deformation of the cantilever at any given time step and the various structural forces acting on it. All these forces counter-balance the external electrostatic pressure and the external acceleration. A self-consistent final state is reached for each time step.

The mechanical deformation of the MEM structure due to the electrostatic forces is obtained by performing 2-D geometrically non-linear analysis of the microstructure. The transient governing equations for an elastic body using a Lagrangian description are given by [6]

$$\mathbf{R_M} = \rho\ddot{\mathbf{u}} + c\dot{\mathbf{u}} - \nabla\cdot(\mathbf{FS}) - \mathbf{B} = 0 \quad in \quad \Omega \quad (1)$$

$$\mathbf{R_M} = \mathbf{u} - \mathbf{G} = 0 \quad on \quad \Gamma_g \quad (2)$$

$$\mathbf{R_M} = \mathbf{P}\cdot\mathbf{N} - \mathbf{H} = 0 \quad on \quad \Gamma_h \quad (3)$$

$$\mathbf{u}|_{t=0} = \mathbf{G_0} \quad in \quad \Omega \quad (4)$$

$$\dot{\mathbf{u}}|_{t=0} = \mathbf{V_0} \quad in \quad \Omega \quad (5)$$

where ρ and c are the material density and material damping factor. $\mathbf{F}$ is the deformation gradient, $\mathbf{u}$, $\dot{\mathbf{u}}$ and $\ddot{\mathbf{u}}$ are the displacement, velocity and acceleration vectors, respectively, $\mathbf{N}$ is the unit outward normal vector in the initial configuration, $\mathbf{S}$ is the second Piola-Kirchhoff stress, $\mathbf{G}$ is the prescribed displacement, $\mathbf{B}$ is the body force term, $\mathbf{G_0}$ and $\mathbf{V_0}$ are the initial displacement and velocity, respectively, $\mathbf{H}$ is the electrostatic pressure acting on the surface of the structures and $\mathbf{P}$ is the first Piola-Kirchhoff stress tensor. $\mathbf{R_M}$ denotes the mechanical residual term in the Newton method. A Newmark scheme [7] with an implicit trapezoidal rule is used for solving the dynamic problem of the nonlinear elastic domain. Numerical discretization is done using the FCM method (see [8] for details on FCM). The 2D governing equation for electrostatic analysis can be written in a Lagrangian boundary integral form as [1], [2]

$$\mathbf{R_{E1}} = \phi(p(P)) - C - \int_{d\Omega} \frac{1}{\epsilon} G(p(P), q(Q))\sigma(q(Q))\mathbf{J}(Q)d\Gamma_Q = 0 \quad (6)$$

$$\mathbf{R_{E2}} = \int_{d\Omega} \sigma(q(Q))\mathbf{J}(Q)d\Gamma_Q - C_T = 0 \quad (7)$$

$$\mathbf{J}(Q) = [\mathbf{T}(Q)\cdot\mathbf{C}(Q)\mathbf{T}(Q)]^{\frac{1}{2}} \quad (8)$$

where ϵ is the dielectric constant of the medium, P and Q are the source and field points in the initial configuration corresponding to the source and field points p and q in the deformed configuration and G is the Green's function. In two dimensions, $G(p,q) = -ln|p-q|/2\pi$, where $|p-q|$ is the distance between the source point p and the field point q. C_T is the total charge of the system and C is an unknown variable which can be used to compute the potential at infinity. $\mathbf{T}(Q)$ is the tangential unit vector at field point Q and $\mathbf{C}(Q)$ is the Green deformation tensor. $\mathbf{R_{E1}}$ and $\mathbf{R_{E2}}$ denotes the electrical residue terms in the Newton step. The electrostatic pressure can be computed from the surface charge density by the relation $\mathbf{H} = P_e J\mathbf{F}^{-T}\mathbf{N}$ where P_e is the electrostatic pressure normal to the surface given by $P_e = \frac{\sigma^2}{2\epsilon}$ and $J = det(\mathbf{F})$. BCM is used for the numerical discretization of the electrostatic boundary integral equations (see [9] for details on BCM).

The main step in the Newton method is the computation of the Jacobian matrix, $\bar{\mathbf{J}}(\mathbf{u},\sigma,C)$, which for the coupled domain MEM problem is

$$\bar{\mathbf{J}}(\mathbf{u},\sigma,C) = \begin{bmatrix} \frac{\partial\mathbf{R_M}}{\partial\mathbf{u}} & \frac{\partial\mathbf{R_M}}{\partial\sigma} & \frac{\partial\mathbf{R_M}}{\partial C} \\ \frac{\partial\mathbf{R_{E1}}}{\partial\mathbf{u}} & \frac{\partial\mathbf{R_{E1}}}{\partial\sigma} & \frac{\partial\mathbf{R_{E1}}}{\partial C} \\ \frac{\partial\mathbf{R_{E2}}}{\partial\mathbf{u}} & \frac{\partial\mathbf{R_{E2}}}{\partial\sigma} & \frac{\partial\mathbf{R_{E2}}}{\partial C} \end{bmatrix} \quad (9)$$

and the residual (right-hand-side), $\mathbf{r}(\mathbf{u},\sigma,C)$, is given by

$$\mathbf{r}(\mathbf{u},\sigma,C) = -\begin{Bmatrix} \mathbf{R_M}(\mathbf{u},\sigma,C) \\ \mathbf{R_{E1}}(\mathbf{u},\sigma,C) \\ \mathbf{R_{E2}}(\mathbf{u},\sigma,C) \end{Bmatrix} \quad (10)$$

The nonlinear mechanical residual equation $\mathbf{R_M}$ can be constructed from Equations (1-5) and its derivatives can be computed in a straight forward manner (see [4], [10] for details). The electrical residual equations for the full-Lagrangian method can be constructed from Equations(6-7). Since the domain of integration is constant (not a function of the displacement $\mathbf{u}$ as in the semi-Lagrangian approach), when computing the terms $\partial\mathbf{R_{E1}}/\partial\mathbf{u}$ and $\partial\mathbf{R_{E2}}/\partial\mathbf{u}$ in $\bar{\mathbf{J}}(\mathbf{u},\sigma,C)$, the integration operator can be taken out of the differentiation operator and the derivatives with respect to $\mathbf{u}$ can be computed directly in the full-Lagrangian approach. This is a major advantage of the full-Lagrangian method over the semi-Lagrangian approach. Algorithm 1 shows the implementation of the Newton based full-Lagrangian method with reference to the two conductor system shown in Figure 2. Ω_1 and Ω_2 denote the original geometries, $d\Omega_1$ and $d\Omega_2$ denote the original surfaces. ω_1 and ω_2 denotes the deformed shapes of conductors 1 and 2, $d\omega_1$ and $d\omega_2$ denote the deformed surfaces. In Algorithm 1, the index n

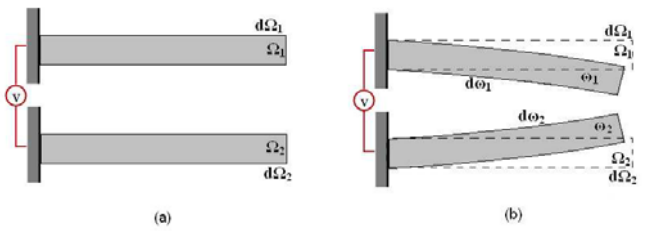

Figure 2: A two conductor electrostatic system.

stands for time instant whereas the index i denotes the i^{th} relaxation iteration within the time step n.

Algorithm 1 Algorithm for the full-Lagrangian based Newton scheme.

1. Discretize Ω_1, Ω_2 for FCM analysis
2. Compute FCM interpolation functions for Ω_1, Ω_2
3. Discretize $d\Omega_1$, $d\Omega_2$ for BCM analysis
4. Compute BCM interpolation functions for $d\Omega_1$, $d\Omega_2$
5. Initialize: $n = 0$, $t_n = \mathbf{u}(t_n) = \dot{\mathbf{u}}(t_n) = \sigma(t_n) = C(t_n) = 0$
6. Compute $\ddot{\mathbf{u}}(t_n)$ from Eqn. (1)
7. For time steps $n = 0, 1, 2, ..., N$:

7(a). Set $i = 0$, $\mathbf{u}(t^i_{n+1}) = \mathbf{u}(t_n)$, $\sigma(t^i_{n+1}) = \sigma(t_n)$, $C(t^i_{n+1}) = C(t_n)$

repeat

i. Compute $\mathbf{T}$, $\mathbf{C}$ and $\mathbf{J}$ from $\mathbf{u}(t^i_{n+1})$

ii. Compute $\bar{\mathbf{J}}(\mathbf{u}(t^i_{n+1}), \sigma(t^i_{n+1}), C(t^i_{n+1}))$ and $\mathbf{r}(\mathbf{u}(t^i_{n+1}), \sigma(t^i_{n+1}), C(t^i_{n+1}))$

iii. Solve:$\bar{\mathbf{J}}[\Delta\mathbf{u}(t^i_{n+1})\ \Delta\sigma(t^i_{n+1})\ \Delta C(t^i_{n+1})]^T$=$\mathbf{r}$

iv. Update $\mathbf{u}(t^{i+1}_{n+1}) = \mathbf{u}(t^i_{n+1}) + \Delta\mathbf{u}(t^i_{n+1})$, $\sigma(t^{i+1}_{n+1}) = \sigma(t^i_{n+1}) + \Delta\sigma(t^i_{n+1})$ and $C(t^{i+1}_{n+1}) = C(t^i_{n+1}) + \Delta C(t^i_{n+1})$

v. Update $i = i + 1$

until a self-consistent final stage is reached

7(b). Update: $\mathbf{u}(t_{n+1}) = \mathbf{u}(t^{i+1}_{n+1})$, $\sigma(t_{n+1}) = \sigma(t^{i+1}_{n+1})$, $C(t_{n+1}) = C(t^{i+1}_{n+1})$

7(c). Compute $\dot{\mathbf{u}}(t_{n+1})$ and $\ddot{\mathbf{u}}(t_{n+1})$ from $\mathbf{u}(t_{n+1})$ (Newmark Scheme)

8. End of for loop for n.

3 RESULTS

The first example is an undamped fixed-fixed beam ($80\mu m$ by $0.5\mu m$ by $10\mu m$), $0.7\mu m$ above a ground plane. A Young's modulus of $169GPa$, density of $2231kg/m^3$ and a Poisson's ratio of 0.3 are employed in the simulations. Figure 3 shows the dynamic pull-in of the fixed-fixed beam for an applied voltage of 15.7V which is close to the published data in [11] of 15.17V. Figure 4 shows that the relaxation method converges slowly compared to the Newton method for the static analysis of the beam

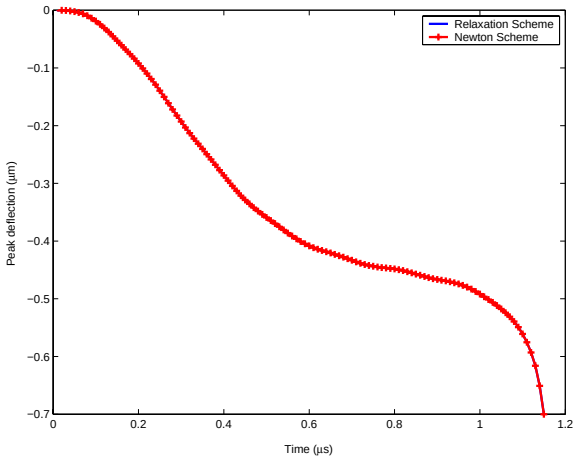

Figure 3: Dynamic analysis of a fixed-fixed beam, for an applied voltage of 15.7V (pull-in).

at an applied voltage of 15V.

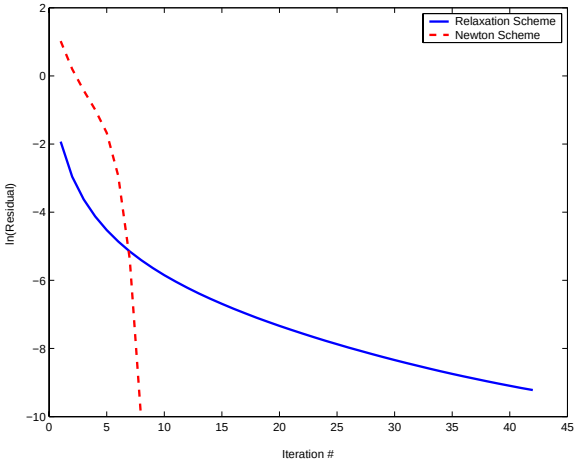

Figure 4: Convergence of the full-Lagrangian Relaxation and Newton methods.

The dynamic characteristics of a transverse comb microactuator (see [12] for details of the comb-drive) is simulated. Figure 5 shows the variation of the resonant frequency of the comb drive with the applied DC bias. The device exhibits spring-softening phenomena due to the electrical forces and it also indicates that mechanical non-linearity which gives rise to spring-hardening is absent. Figure 6 shows the frequency response curve of the device for a 2.5V DC bias and a 5V p-p AC bias at various frequencies. Interestingly, two resonant peaks are observed instead of the conventional single peak at the resonant frequency. The second peak, observed at half of the natural frequency is due to the V^2 nature of the electrostatic force.

A lateral comb drive (see [13] for details of the comb-

drive) actuator is also simulated with the Newton method. Simulations show that the resonant frequency of the comb drive remains constant at 74 KHz with the applied DC bias, which is very close to the experimentally measured value of 75 KHz. The constant resonant frequency (independent of applied voltage) is due to the fact that the electrostatic force is not a function of the displacement x and hence there is no spring-softening effect. Figure 7 shows the frequency response curve of the device for a 200V DC bias and a 200V p-p AC bias at various frequencies. Two resonant peaks are observed again, one at the resonant frequency of 74 KHz and the other at 34 KHz, which is approximately half of the first resonant frequency.

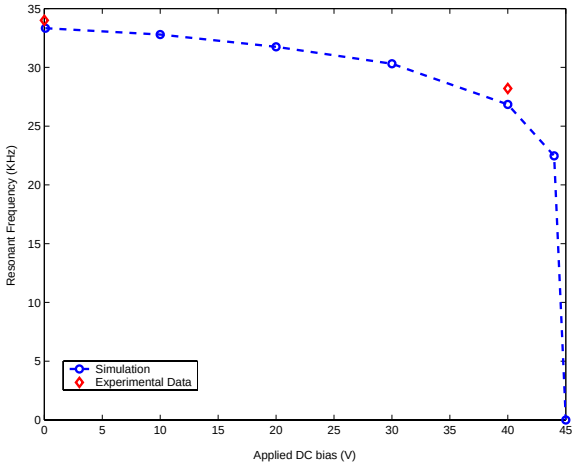

Figure 5: Variation of resonant frequency with applied DC bias.

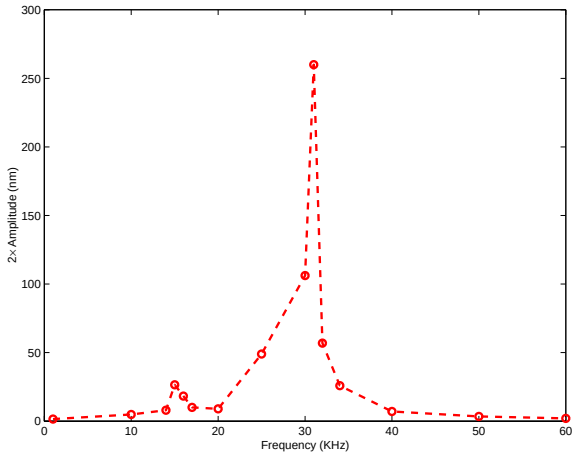

Figure 6: Frequency response of the transverse comb drive.

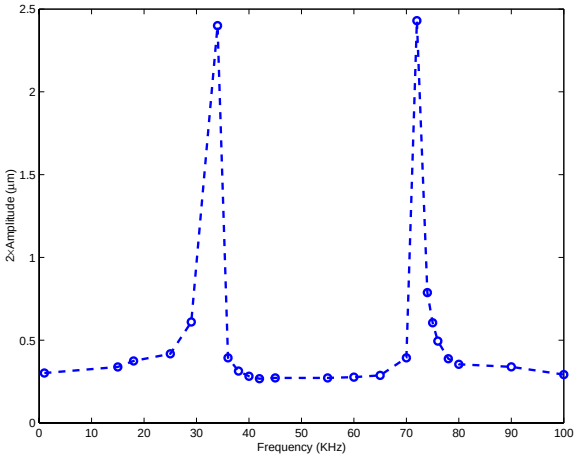

Figure 7: Frequency response of the lateral comb drive.

4 CONCLUSIONS

Full-Lagrangian based Newton scheme has been developed in this paper for the dynamic analysis of MEMS. The full-Lagrangian method exhibits excellent convergence rates and greatly improves the performance of the dynamic analysis by eliminating time consuming steps like recomputing the interpolation functions and re-discretization of the surfaces and by accurate computation of the Jacobian matrix. The Newton method has been successfully applied for the dynamic analysis of complex comb-drive MEM structures.

REFERENCES

[1] G. Li, et. al., JMEMS, 11(3), 45-254, 2002.
[2] G. Li, et. al., IEEE-TCAD, 22(9), 1228-1242, 2003.
[3] S. D. Senturia, et. al., JMEMS, 1(1), 3-13, 1992.
[4] N. R. Aluru, et. al., Sensors and Actuators A, 58, 1-11, 1997.
[5] N. R. Aluru, et. al., JMEMS, 8(3), 299-308, 1999.
[6] D. S. Chandrasekharaiah, et. al., "Continuum Mechanics", Academic Press, 1994.
[7] K. J. Bathe, "Finite Element Procedures", Prentice-Hall, 1995.
[8] X. Jin, et. al., CMES, 2(4), 447-462, 2001.
[9] G. Li, et. al., Engr. Analysis with Boundary Elements, 27(1), 57-71, 2003.
[10] S. K. De, et. al., JMEMS, submitted for publication.
[11] G. K. Ananthasuresh, et. al., ASME Dynamic Systems and Control (DSC) Series, 59, 401-407, 1996.
[12] T. Imamura, et. al., IEEE/ASME Trans. on Mechantronics, 3(3), 166-174, 1998.
[13] W. C. Tang, et. al., Procs. of Micro Electro Mechanical Systems, 53-59, 1989.